Oecologia (2007) 151:54–68
DOI 10.1007/s00442-006-0565-2

ECOSYSTEM ECOLOGY

Coupling between carbon cycling and climate in a high-elevation, subalpine forest: a model-data fusion analysis

William J. Sacks · David S. Schimel · Russell K. Monson

Received: 11 February 2006 / Accepted: 29 August 2006 / Published online: 30 September 2006

Abstract Fundamental questions exist about the effects of climate on terrestrial net ecosystem CO_2 exchange (NEE), despite a rapidly growing body of flux observations. One strategy to clarify ecosystem climate–carbon interactions is to partition NEE into its component fluxes, gross ecosystem CO_2 exchange (GEE) and ecosystem respiration (R_E), and evaluate the responses to climate of each component flux. We separated observed NEE into optimized estimates of GEE and R_E using an ecosystem process model combined with 6 years of continuous flux data from the Niwot Ridge AmeriFlux site. In order to gain further insight into the processes underlying NEE, we partitioned R_E into its components: heterotrophic (R_H) and autotrophic (R_A) respiration. We were successful in separating GEE and R_E, but less successful in accurately partitioning R_E into R_A and R_H. Our failure in the latter was due to a lack of adequate contrasts in the assimilated data set to distinguish between R_A and R_H. We performed most model runs at a twice-daily time step. Optimizing on daily-aggregated data severely degraded the model's ability to separate GEE and R_E. However, we gained little benefit from using a half-hourly time step. The model-data fusion showed that most of the interannual variability in NEE was due to variability in GEE, and not R_E. In contrast to several previous studies in other ecosystems, we found that longer growing seasons at Niwot Ridge were correlated with *less* net CO_2 uptake, due to a decrease of available snow-melt water during the late springtime photosynthetic period. Warmer springtime temperatures resulted in increased net CO_2 uptake only if adequate moisture was available; when warmer springtime conditions led into mid-summer drought, the annual net uptake declined.

Keywords Ecosystem respiration · Eddy covariance · Gross primary productivity · Net ecosystem exchange · Parameter estimation

Communicated by Jim Ehleringer.

W. J. Sacks (✉)
Center for Sustainability and the Global Environment,
Nelson Institute for Environmental Studies,
University of Wisconsin-Madison, 1710 University Avenue,
Madison, WI 53726, USA
e-mail: wsacks@wisc.edu

W. J. Sacks · D. S. Schimel
National Center for Atmospheric Research,
1850 Table Mesa Drive, Boulder, CO 80305, USA

R. K. Monson
Department of Ecology and Evolutionary Biology
and Cooperative Institute for Research
in the Environmental Sciences,
University of Colorado, Boulder,
CO 80309-0334, USA

Introduction

Correlations between climate and CO_2 exchange at local to global scales provide information about climate controls over terrestrial carbon cycling (Goulden et al. 1996; Angert et al. 2005; Ciais et al. 2005; Sacks et al. 2006). Despite a growing body of literature in these areas, fundamental questions remain about the separate and interactive effects of temperature, water and other climate variables on terrestrial ecosystems (Breshears et al. 2005). Particularly problematic is the fact that net ecosystem CO_2 exchange (NEE) reflects

the small difference between the opposing large CO_2 fluxes of gross ecosystem exchange (GEE) and ecosystem respiration (R_E), fluxes that tend to respond similarly but not identically to the environment. Predicting the terrestrial carbon response to climate variables requires precise prediction of the differential effects of climate on GEE and R_E and their interactions, together with the localized but large effects of disturbance. Small errors in the climate sensitivity of the GEE and R_E fluxes, or the time scale on which they respond, can cause major errors in NEE. Modeling of NEE in large scale has proved challenging, and models based on similar principles give contrasting results. This is partly because of the difficulty of precise estimation of parameters governing these fluxes in noisy and heterogeneous systems, and partly because GEE and R_E are not independent, but rather linked by substrate production and use, and by their common dependence on nutrient availability (Ryan and Law 2005).

In theory, diagnosis of environmental controls on NEE should be feasible using long-term eddy covariance measurements—these fluxes contain the relevant responses of photosynthesis and respiration to the environment, and these measurements are made at a high density capable of revealing fine-grained patterns in a long time series. However, direct flux measurements do not solve the parametric problem for prediction because the component processes (GEE and R_E) must be inferred a priori from the flux data, i.e., before parameter values can be estimated. This problem of circularity is in principle similar to other problems in the Earth sciences where understanding an observed phenomenon requires inference of real but unobservable component quantities. The problem can be addressed by combining the observations with a model of the underlying processes to produce an analysis of the indirectly observed fluxes consistent with both theory (via the model) and observations (via the data).

In past studies, we addressed the problems of parameter estimation using a powerful model-data fusion approach (Braswell et al. 2005; Sacks et al. 2006; see also Schulz et al. 2001; Wang et al. 2001; Raupach et al. 2005; Williams et al. 2005). This approach addresses the interactive nature of GEE and R_E through modeled recognition of their substrate-level controls. The model-data fusion yields a model for which the parameters are consistent with both prior knowledge of physiology and the observed patterns of NEE, as realized over all seasons and multiple years. Combining the model and observations in this way produces a theoretically accurate and highly constrained analysis of NEE, including its dependence on the responses of photosynthesis, and the responses of heterotrophic and autotrophic respiration to seasonal and interannual environmental variability.

In this study, we applied the model-data fusion approach to the 6-year Niwot Ridge AmeriFlux data record, which includes continuous eddy covariance fluxes and other ecological measurements (Monson et al. 2002; Turnipseed et al. 2002, 2003; Scott-Denton et al. 2003, 2006; Monson et al. 2005). The site is characterized by snow-covered winters, a spring-time melt season and a dry summer season with episodic and variable rains. Much of the net CO_2 uptake occurs during the period when soil moisture is provided by snow-melt (Monson et al. 2002, 2005). From the existing research record, it appears that a number of factors control the annual balance of GEE and R_E. The timing and depth of winter snow regulates winter snow cover and affects soil temperatures through insulation. The timing and duration of the snow-melt period influences when springtime photosynthesis begins and for how long it proceeds before water stress reduces it. The amount of summer rain affects both GEE andR_E after the snow-melt moisture is gone. While qualitative and, to a certain extent, quantitative inferences about GEE and R_E can be made from such observations, we processed this record using a model-data fusion analysis to arrive at quantitative estimates of the sensitivity of GEE and R_E to temperature, moisture and other variables consistent with the patterns observed above.

Materials and methods

Study site

The Niwot Ridge AmeriFlux Site is located approximately 50 miles west of Boulder, Colorado (40°1′58″N; 105°32′47″W) at 3,050 m elevation. The site is situated in the subalpine forest ecosystem with the dominant species being *Abies lasiocarpa* (subalpine fir), *Picea engelmannii* (Engelmann spruce) and *Pinus contorta* (lodgepole pine). The forest is accumulating carbon, recovering from logging that ended about 100 years ago (Monson et al. 2002). The canopy at the site is relatively open, with an average gap fraction of 17% (Turnipseed et al. 2003). The average canopy height is 11.4 m and average mid-summer leaf-area index is 4.2 m^2 m^{-2} (Monson et al. 2002; Turnipseed et al. 2002). The site has a sparse, heterogeneous ground cover, mostly composed of *Vaccinium* sp., lichens and occasional moss. Soils are sandy and derived from granitic moraine with a distinct, thin (<6 cm) organic

horizon. Mean annual precipitation at the site is 800 mm, and the mean annual temperature is 1.5°C.

Measurements of NEE and associated meteorological parameters

From November 1998 through the present, fluxes of CO_2, sensible and latent heat, and a number of meteorological variables have been measured as part of the Niwot Ridge AmeriFlux program (http://urquell.colorado.edu/data_ameriflux/). For this study, we used data from 1 November 1998 through 31 December 2004. CO_2 fluxes were measured using the eddy covariance method. General details of the eddy covariance approach are provided by Baldocchi (2003), and specific details for measurements at the Niwot Ridge AmeriFlux site are provided in several previous reports (Monson et al. 2002; Turnipseed et al. 2002, 2003, 2004). Briefly, turbulent fluxes were measured using a triaxial sonic anemometer (SWS-211/3 K, Applied Technologies, Inc., Boulder CO, USA) and a closed-path infrared gas analyzer (Li-Cor 6262, Li-Cor Inc, Lincoln NE, USA). Measurements were aligned with the mean wind streamlines (Kaimal and Finnigan 1994), and standard density corrections (Webb et al. 1980) were applied. Beneath-canopy CO_2 storage was determined by vertical integration of six profile stations located on the tower and added to the eddy-flux measurement to compute the overall NEE as described in Goulden et al. (1996). By convention, net CO_2 fluxes are referenced to the atmosphere: negative fluxes represent CO_2 loss from the atmosphere (net ecosystem photosynthesis) and positive fluxes represent CO_2 gain by the atmosphere (net ecosystem respiration).

Air temperatures were determined from the temperature signal of the sonic anemometer at the same height (21.5 m) as the turbulent flux measurements. Soil temperatures were averaged over the top 10 cm of soil. Precipitation values were acquired from the University of Colorado Long-Term Ecological Research web site (http://culter.colorado.edu). These values had been obtained from standard precipitation gauge measurements at a site 500 m north of the tower flux site.

Gaps occur in the flux and meteorological measurements due to instrument malfunction or, in the case of fluxes, periods of high atmospheric stability (which can cause an underestimate of the flux; Goulden et al. 1996; Monson et al. 2002). These gaps were filled using a variety of methods, depending on the length of the gap: spline fits, averages of the surrounding days, or empirical regressions based on the available meteorological data (Monson et al. 2002). Because the ecosystem model was normally run using two time steps per day (day and night), we aggregated the half-hourly averaged data up to these time steps, using the gap-filled data where necessary. To minimize the effect of fitting the model to already modeled ''data'', only twice-daily time steps that contained at least 50% measured (i.e., not gap-filled) half-hourly fluxes were included in the optimization (we call these ''valid'' data points). This led to the exclusion of 23% of the twice-daily observations from the optimization. We chose not to use a more conservative cut-off, because doing so would also have led to the exclusion of more measured data points (but see Braswell et al. 2005 for a discussion of the sensitivity of the parameter estimation to the cut-off criterion). For example, requiring all half-hourly measurements making up a time step to be non-gap-filled would mean that 70% of the time steps would have been excluded.

The SIPNET ecosystem model

The SIPNET model was designed to simulate the most significant controls over variability in CO_2 fluxes, including the diurnal cycle, while keeping the model as simple as possible (Braswell et al. 2005; Sacks et al. 2006). Using a simple model reduces the number of parameters, thus helping avoid the danger of over-fitting the observations during the optimization and also reducing the computational intensity of the optimization. The model is, for the most part, a simplified version of the PnET (Photosynthesis-EvapoTranspiration) model (Aber and Federer 1992; Aber et al. 1995, 1996, 1997); acknowledging the contributions of the PnET model, we refer to our version as SIPNET (for Simplified PnET).

SIPNET describes carbon flux dynamics in two vegetation carbon pools and an aggregated soil carbon pool (Fig. 1). To model biomass partitioning and respiration, the vegetation was split into leaves and wood, where ''wood'' refers to the combined pool of boles, branches and roots. For most model runs, we used SIPNET with twice-daily daytime and nighttime time steps. The lengths of the day and night time steps were varied seasonally to account for changes in day length; fluxes were appropriately scaled for these changes. In each step, six climate variables drove the flux dynamics: (1) average air temperature (T_{air}), (2) average soil temperature (T_{soil}), (3) precipitation, (4) flux density of photosynthetic photon flux density (PPFD), (5) relative humidity, and (6) wind speed. Atmospheric vapor pressure and vapor pressure deficit (VPD) were then computed from relative humidity and air temperature. The model's dynamics were governed by the values of 32 parameters, 17 of which were allowed to vary in the

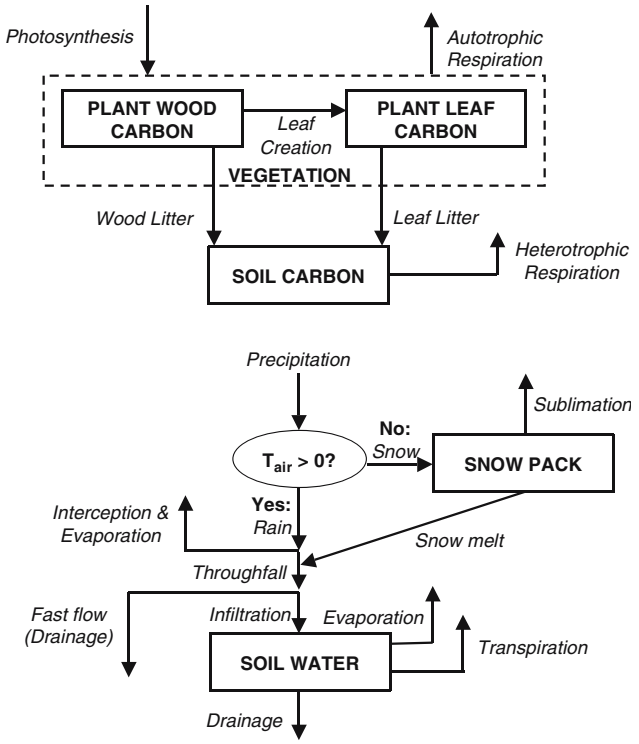

Fig. 1 SIPNET pools and fluxes. The model has two vegetation carbon pools and one soil carbon pool. The soil moisture submodel includes a single soil moisture pool and a snow pack. Soil moisture affects both photosynthesis and soil respiration, as described in the text

optimization (Table 1), and 15 of which were fixed at values from the literature or from field studies at Niwot Ridge (Table 2).

There are six carbon fluxes in SIPNET: (1) GEE, which is synonymous with gross primary productivity and gross photosynthesis, (2) autotrophic respiration (R_A), (3) heterotrophic respiration (R_H), (4) new leaf growth, (5) formation of leaf litter, and (6) formation of wood litter. We used the same formulation for calculating GEE as that used in PnET (Aber and Federer 1992):

$$\mathrm{GEE_{pot}} = \mathrm{GEE_{max}} D_{\mathrm{temp}} D_{\mathrm{VPD}} D_{\mathrm{light}} \quad (1)$$

where $\mathrm{GEE_{pot}}$ is the potential gross photosynthetic rate per unit leaf mass, without water stress; $\mathrm{GEE_{max}}$ is the daily maximum gross photosynthetic rate, calculated from the parameters $A_{\max}$, F_{Amax} and K_F; and D_{temp}, D_{VPD} and D_{light} are scalars that take on values between 0 and 1 and represent decreases in photosynthesis due to temperature, vapor pressure deficit and light. D_{light} was computed by approximating the integral through the canopy, considering six vertical layers and computing $D_{\mathrm{light},i}$ for each of these layers. These three scalars were calculated as:

$$D_{\mathrm{temp}} = \mathrm{Max}\left(\frac{(T_{\max} - T_{\mathrm{air}})(T_{\mathrm{air}} - T_{\min})}{(T_{\mathrm{opt}} - T_{\min})^2}, 0\right) \quad (2a)$$

$$D_{\mathrm{VPD}} = 1 - K_{\mathrm{VPD}}\mathrm{VPD}^2 \quad (2b)$$

$$D_{\mathrm{light},i} = 1 - \mathrm{e}^{-(I_i \ln(2)/\mathrm{PPFD}_{1/2})} \quad (2c)$$

where $T_{\max}$ was computed as $T_{\mathrm{opt}}+(T_{\mathrm{opt}}-T_{\min})$, I_i is the light intensity at a given layer i, computed using Beer's Law, and other parameters are as defined in Table 1.

$\mathrm{GEE_{pot}}$, along with the plants' water use efficiency (WUE), was then used to calculate potential transpiration (T_{pot}), as:

$$\mathrm{WUE} = \frac{K_{\mathrm{WUE}}}{\mathrm{VPD}} \quad (3a)$$

$$T_{\mathrm{pot}} = \frac{\mathrm{GEE_{pot}}}{\mathrm{WUE}} \quad (3b)$$

Plant-available soil water was computed using the parameter f, and actual transpiration (T) was set to the lesser of T_{pot} and plant-available water. Finally, GEE was computed using:

$$D_{\mathrm{water}} = \frac{T}{T_{\mathrm{pot}}} \quad (4a)$$

$$\mathrm{GEE} = \mathrm{GEE_{pot}} D_{\mathrm{water}} \quad (4b)$$

Autotrophic respiration is the sum of foliar and wood respiration. To keep the model simple, we aggregated growth and maintenance respiration. Foliar and wood respiration were both modeled as:

$$R_x = K_x C_x Q10_V^{T_{\mathrm{air}}/10} \quad (5)$$

where R_x is the realized respiration rate, K_x is a base rate, C_x is the carbon in the given pool (either wood or leaves), and $Q10_V$ is the parameter governing the increase in autotrophic respiration for every 10° increase in temperature.

Heterotrophic respiration represents the respiration of microbes in the model's single aggregated soil pool. In addition to a temperature effect similar to that governing autotrophic respiration, heterotrophic respiration also increased linearly with soil moisture:

$$R_H = K_H C_S Q10_S^{T_{\mathrm{soil}}/10}\left(\frac{W_S}{W_{S,c}}\right) \quad (6)$$

where C_S is soil carbon content, W_S is soil water content, and other parameters are as defined in Table 1.

Table 1 SIPNET parameters and initial conditions that were allowed to vary in the optimization, and their allowable ranges

Symbol	Definition	Range
Initial pool values		
$W_{S,0}$	Initial soil moisture content (fraction of $W_{S,c}$)	0–1
Photosynthesis/respiration parameters		
A_{max}	Maximum net CO_2 assimilation rate [nmol CO_2 g^{-1} (leaf biomass) s^{-1}]	0–34
T_{min}	Minimum temperature for photosynthesis (°C)	–8 to 8
T_{opt}	Optimum temperature for photosynthesis (°C)	5–30
K_{VPD}	Slope of VPD-photosynthesis relationship (kPa^{-1})	0.01–0.25
$PPFD_{1/2}$	Half saturation point of PPFD-photosynthesis relationship (mol m^{-2} day^{-1})	4–27
K_F	Foliar maintenance respiration as fraction of A_{max} (no units)	0.05–0.30
K_A	Wood respiration rate at 0°C (g C g^{-1} C $year^{-1}$)	0.0006–0.06
$Q10_V$	Vegetation respiration Q_{10} (no units)	1.4–2.6
T_s	Soil temperature at which photosynthesis and foliar respiration are shut down (°C)	–5 to 5
K_H	Soil respiration rate at 0°C and moisture-saturated soil (g C g^{-1} C $year^{-1}$)	0.003–0.6
$Q10_S$	Soil respiration Q_{10} (no units)	1.4–5
Water-related parameters		
F	Fraction of soil water removable in 1 day (no units)	0.001–0.16
K_{WUE}	VPD-water use efficiency relationship (mg CO_2 kPa g^{-1} H_2O)	0.01–109
$W_{S,c}$	Soil water holding capacity (cm precipitation equivalent)	0.1–36
R_d	Scalar relating aerodynamic resistance to wind speed (no units)[a]	1–1,500
Tree physiological parameters		
NPP_L	Fraction of NPP allocated to leaf growth (no units)	0–1

The ranges assume a uniform prior distribution

[a] $r_d=R_d/u$ (r_d=aerodynamic resistance, u=wind speed)

Table 2 SIPNET parameters and initial conditions that were held constant in the optimization

Symbol	Definition	Value	Source[a]
Initial pool values			
$C_{W,0}$	Initial plant wood C content (g C m^{-2})	9,600	*RM*
$C_{L,0}$	Initial leaf area index (m^2 m^{-2})	4.2	*M02*
$C_{S,0}$	Initial soil C content (organic layer only) (g C m^{-2})	16,000	*S03*
$W_{P,0}$	Initial snow pack (cm water equivalent)	0	NA
Photosynthesis/respiration parameters			
F_{Amax}	Average daily max photosynthesis as fraction of A_{max} (no units)	0.76	*A96*
K	Canopy PPFD extinction coefficient (no units)	0.5	*A96*
Water-related parameters			
E	Fraction of rain immediately intercepted and evaporated (no units)	0.1	*A92*
F	Fraction of water entering soil that goes directly to drainage (no units)	0.1	*A92*
K_S	Snow-melt rate [cm (water equivalent) $°C^{-1}$ day^{-1}]	0.15	*A92*
$R_{soil,1}$	Scalar relating soil resistance to soil wetness (see text) (no units)	8.2	*S96*
$R_{soil,2}$	Scalar relating soil resistance to soil wetness (see text) (no units)	4.3	*S96*
Tree physiological parameters			
SLW_C	C content of leaves on a per-area basis [g C m^{-2} (leaf area)]	270	*JS*
F_C	Fractional C content of leaves [g C g^{-1} (leaf biomass)]	0.45	*A95*
K_L	Turnover rate of leaf C (g C g^{-1} C $year^{-1}$)	0.13	*LS*
K_W	Turnover rate of plant wood C (g C g^{-1} C $year^{-1}$)	0.014	*PT*

Most of these parameters were highly correlated with other parameters in the model and, thus, could not be estimated independently

[a] Sources are: *A92*, Aber and Federer (1992); *A95*, Aber et al. (1995); *A96*, Aber et al. (1996); *JS*, J. Sparks, unpublished data; *LS*, L. Scott-Denton, unpublished data; *M02*, Monson et al. (2002); *PT*, P. Thornton, personal communication, 1/21/05; *RM*, R. Monson, unpublished data; *S96*, Sellers et al. (1996); *S03*, Scott-Denton et al. (2003)

The forest in the footprint of the flux tower is dominated by evergreen vegetation, and so we assumed an evergreen phenology. In each time step, leaf carbon was added at a rate proportional to the mean net primary productivity over the previous 5 days, and carbon was lost from the leaves (and added to the soil)

at a constant rate. Wood litter was also modeled using a constant turnover rate.

Photosynthesis in cold climates is drastically reduced when the soil is frozen; a suggested mechanism involves the shutdown of water flow in frozen soils (Hollinger et al. 1999; Monson et al. 2002). Because there is little or no fresh photosynthate supplied to the leaves at this time, it is likely that foliar respiration is also reduced to near-zero. We incorporated these controls into SIPNET by shutting down photosynthesis and foliar respiration when the soil temperature was below a given threshold. Sacks et al. (2006) found that this wintertime downregulation of photosynthesis and foliar respiration improved the model's ability to match observations of NEE.

At Niwot Ridge, water stress is one of the largest determinants of NEE (Monson et al. 2002). In this study, in contrast to that performed by Sacks et al. (2006), we used a single soil water pool for both evaporation and transpiration, because the CO_2 flux data do not contain enough information to constrain the soil moisture dynamics of a model with two water pools (Sacks et al. 2006). In fact, we found that using an additional water pool actually led to a slightly degraded model-data fit.

Evaporation from the soil (E_S) and sublimation from the snow pack (E_P) were modeled as in the SiB2 model (Sellers et al. 1996):

$$\lambda E_S = \frac{e^*(T_{soil}) - e_a}{r_{soil} + r_d} \frac{\rho c_p}{\gamma} \tag{7a}$$

$$\lambda_s E_P = \frac{e^*(0^\circ C) - e_a}{r_d} \frac{\rho c_p}{\gamma} \tag{7b}$$

where λ is the latent heat of vaporization, λ_s is the latent heat of sublimation, $e^*(T)$ is the saturation vapor pressure at temperature T, e_a is the atmospheric vapor pressure, ρ is the density of air, c_p is the specific heat of air, γ is the psychrometric constant, r_d is the aerodynamic resistance between the ground and the canopy air space, which decreases linearly with wind speed, and r_{soil} is a soil resistance term, computed as in Sellers et al. (1992):

$$r_{soil} = e^{R_{soil,1} - R_{soil,2}(W_S/W_{S,c})} \tag{8}$$

Finally, transpiration was the smaller of potential transpiration and plant-available soil water, as described above.

Parameter optimization

We used a version of the Metropolis simulated annealing algorithm (Metropolis et al. 1953) to optimize about half of the parameters governing the initial state and time evolution of SIPNET (Table 1). The remaining parameters (Table 2) were held constant at values from the literature or from field studies at Niwot Ridge. These latter parameters were ones that we found, through initial experiments, could not be estimated well, either because of correlations with other parameters or because they had only a weak effect on modeled NEE (Schulz et al. 2001; Wang et al. 2001). For example, most initial pool values could not be estimated independently of the various rate constants because of high correlations between these two sets of parameters. The procedure used for this optimization was essentially the same as that described by Braswell et al. (2005).

The optimization algorithm generates not only a single best parameter set, but also a range of parameter sets that represent approximately equally good matches to the data. This allows the generation of confidence intervals on the optimal parameter values and the determination of correlations between parameters. In addition, by running the model forward on the retrieved ensemble of parameter sets, confidence intervals can be generated on the optimized model output. The full deployment of these features of the optimization is described by Braswell et al. (2005) and not repeated here. Additionally, Braswell et al. (2005) presented an analysis of the parameter optimization given a synthetic data set. This optimization resulted in a generally good match between the retrieved parameters and the true parameters. Experiments with synthetic data demonstrate that the Metropolis algorithm takes the system to the global constrained minimum for this problem.

Initial values and boundaries for the parameters were defined through a combination of literature values, best guesses and actual measurements. Searching the entire parameter space is infeasible, as this space is theoretically infinite. Thus, we bounded each parameter within a range (the "prior distribution") that is biologically or physically possible based on previous knowledge about the process, therefore eliminating solutions that violate prior knowledge. In general, we specified relatively broad parameter boundaries and, in some cases, iteratively increased the boundary widths until the optimized parameter value fell well within the allowable range rather than being on its edge. However, we attempted to avoid making the boundaries so wide that unrealistic estimates for one parameter forced other parameters to take on less realistic values (so, for example, we did not further widen the ranges of $Q10_V$ and $Q10_S$). Thus, the ranges used in the optimization represent an attempt at a compromise:

wide enough that the optimum values for most parameters fall within the specified range, but narrow enough that the ranges exclude parameter values that are grossly unrealistic.

The optimization consisted of performing a quasi-random walk through the multi-dimensional parameter space to find the parameter set that caused the model to generate the best match of predicted NEE (defined as R_A+R_H–GEE) with observed NEE. Although it is possible to use multiple constraints in the optimization (Wang et al. 2001; Williams et al. 2005), for this study we used NEE alone (but see Sacks et al. 2006 for the effects of including water vapor fluxes as an additional constraint). We conducted the analysis across all 6 years of the available NEE data, and for daytime and nighttime points simultaneously, so the optimized parameter set reflects that determined for the entire data set. The ''best match'' is defined as the model output that maximizes likelihood (L):

$$L = \prod_{i=1}^{n} \frac{1}{\sigma\sqrt{2\pi}} e^{-(X_i-\mu_i)^2/2\sigma^2} \quad (9)$$

where n is the number of valid data points, X_i is the eddy covariance-derived NEE summed over time step i (in g C m^{-2}), μ_i is the modeled NEE in time step i (in g C m^{-2}), and σ is the error (one standard deviation) on each data point. Here, σ represents data error *relative to the given model structure* and, thus, represents a combination of measurement error and process representation error. Note, that we assumed that each data point has the same uncertainty and that the deviations from the model predictions are independent over time. In practice, log likelihood is used in place of likelihood because it is computationally easier to work with. Details such as step size and stopping point are discussed by Braswell et al. (2005).

Because we did not have measured values of σ, we treated σ as a parameter to be estimated at each step of the optimization (Hurtt and Armstrong 1996). For a given model output (that is, a given set of μ_i values), the value of σ that maximizes L, which we denote σ_e, is given by:

$$\sigma_e = \sqrt{\frac{1}{n}\sum_{i=1}^{n}(X_i - \mu_i)^2} \quad (10)$$

We then used σ_e in place of σ in the calculation of L. Although this procedure may impact the width of the parameter confidence intervals, it should not significantly impact the retrieved optimum parameter set.

At each step in the optimization, a parameter was chosen at random and its value changed. The optimization then evaluated the likelihood at the new point (by running the model using the newly generated parameter set) and compared it with the likelihood at the old point. If L(new)≥L(old), then the algorithm accepted the new parameter value. If L(new)<L(old), then the probability that the algorithm accepted the new parameter value was given by the ratio of the likelihoods. If the new value was accepted, the algorithm took the next step from this new point. If the new value was rejected, then the algorithm took another random step using the old value. The occasional acceptance of worse points in the parameter space helps prevent the optimization from getting stuck in local, but non-global, optima. After a spin-up period (similar to that described in Braswell et al. 2005), the set of accepted points is an estimator of the posterior distribution of the parameters, and the estimated parameter set that yielded the maximum likelihood across the entire optimization is taken to be the optimal parameter set. We ran the optimization long enough to generate about 150,000 accepted points.

Results

Optimized fluxes

The optimized parameter set is given in Table 3. The posterior distributions of the parameters are also given; the narrow standard deviations of the estimated parameter means show that the parameters were well constrained by the observations. Braswell et al. (2005) and Sacks et al. (2006) discussed the issue of correlations between the different SIPNET parameters; for the present study, we fixed parameters in the optimization if they were highly correlated with another parameter.

The model, post-optimization, matched the general diurnal and seasonal patterns in the observations well (Figs. 2a, 3a, b), and also matched the observed cumulative CO_2 uptake in most years (Fig. 2b). There are a few areas of obvious misfit between model and observations. First, the model underestimated peak nighttime respiration (Fig. 2a), possibly because of microbial community and substrate dynamics that are not represented in SIPNET. Second, the model underestimated peak summertime uptake (Fig. 2a). Third, the model failed to fully capture periods of drought-induced decreases in NEE, such as in mid-summer 2002, when the observations indicated a period of net CO_2 loss from the ecosystem to the

Table 3 Parameter values retrieved from the optimization (see Table 1 for parameter definitions). The ''Best value'' column reports the parameter set that yielded the highest likelihood in the standard (twice-daily) parameter estimation. The ''Mean value'' column reports the estimated posterior mean and standard deviation of each parameter, generated from 150,081 parameter sets that yielded approximately equally good model-data fits. The ''Half-hourly mean'' column reports the estimated mean and standard deviation of each parameter when the model was run and optimized at a half-hourly time step

Parameter	Best value	Mean value	Half-hourly mean
$W_{S,0}$	0.02	0.03±0.01	0.020±0.003
A_{max} (nmol CO_2 g^{-1} s^{-1})	4.79	4.77±0.15	**8.73±0.08**
T_{min} (°C)	–2.97	–3.13±0.20	–2.78±0.09
T_{opt} (°C)	14.3	14.2±0.5	**19.4±0.3**
K_{VPD} (kPa^{-1})	0.127	0.123±0.006	**0.138±0.001**
$PPFD_{1/2}$ (mol m^{-2} day^{-1})	7.4	7.5±0.5	**14.9±0.2**
K_F	0.097	0.100±0.009	**0.064±0.002**
K_A (g C g^{-1} C $year^{-1}$)	0.027	0.028±0.001	0.027±0.001
$Q10_V$	1.40	1.43±0.02	1.46±0.02
T_s (°C)	0.106	0.105±0.002	**–0.002±0.002**
K_H (g C g^{-1} C $year^{-1}$)	0.007	0.006±0.001	**0.0082±0.0002**
$Q10_S$	4.96	4.66±0.28	4.99±0.01
f	0.088	0.075±0.019	0.059±0.002
K_{WUE} (mg CO_2 kPa g^{-1} H_2O)	47.7	59.1±15.2	**106.2±2.6**
$W_{S,c}$ (cm)	4.08	4.03±0.27	**3.46±0.04**
R_d	36.5	36.5±0.9	**33.7±0.3**
NPP_L	0.40	0.41±0.03	0.37±0.01

Values in bold differ from the standard optimization by more than two standard deviations

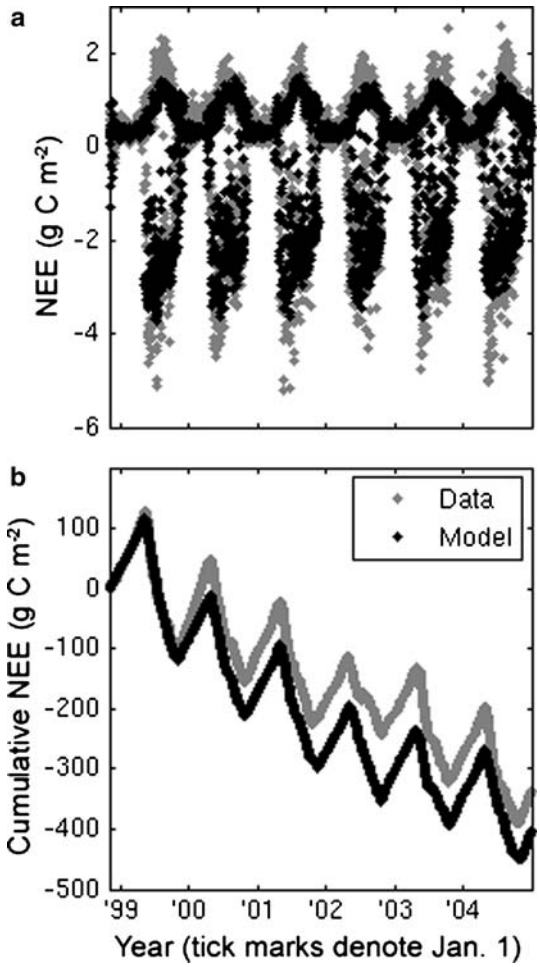

Fig. 2 Twice-daily (day and night separated) time series of modeled and observed NEE (**a**), and cumulative NEE (**b**), from 1 November 1998 through 31 December 2004. Model results were generated using the best parameter set retrieved from the optimization. Positive NEE denotes net loss of CO_2 from the ecosystem to the atmosphere. Major errors between the model and observations are that the model (1) underestimated peak summertime CO_2 uptake, (2) underestimated peak nighttime respiration rates, and (3) did not capture the mid-summer NEE reduction in 2002

atmosphere, yet the model predicted continued CO_2 uptake (Fig. 3a, b). These last two errors may have arisen because the model was unable to capture the proper soil moisture limitation at this site, and had to make a compromise in photosynthetic rates between times of little water stress (e.g., late spring) and times of significant water stress (e.g., mid-summer 2002) (Sacks et al. 2006). However, the overall fit is satisfactory, with a RMS error between model and valid observations of 0.530 g C m^{-2} (daytime points: 0.652 g C m^{-2}; nighttime points: 0.300 g C m^{-2}).

Using the optimized model, we partitioned NEE into its component fluxes, GEE and R_E (Figs. 3c, d, 4a, b). The model predicted mean fluxes (over 1999–2004) of 652 g C m^{-2} $year^{-1}$ for GEE and 579 g C m^{-2} $year^{-1}$ for R_E, with a resulting NEE of –73 g C m^{-2} $year^{-1}$ (the observed mean NEE over this time period was –62 g C m^{-2} $year^{-1}$). The model predicted that the seasonal cycle of NEE is driven primarily by variability in GEE, which had about twice the seasonal range as that of R_E (Fig. 4a). On average, a key switch in the seasonal cycle occurred in May, when a large increase in GEE occurred and the monthly NEE became negative, indicating net CO_2 uptake. GEE continued to increase between May and June, which caused NEE in June to become even more negative. Month-to-month variability in summertime NEE, however, was predicted to be due more to variability in R_E. Predicted R_E reached a maximum in July, whereas GEE remained roughly constant from June through August; this resulted in net CO_2 uptake being somewhat depressed in July relative to the net uptake in other months of the growing season. NEE variability in the fall, like that in the spring, was governed more strongly by variability in GEE. A large decrease in GEE in November, relative to that in October, caused NEE to become positive in this month. In the winter, there was little month-to-month variability in either the net or gross fluxes.

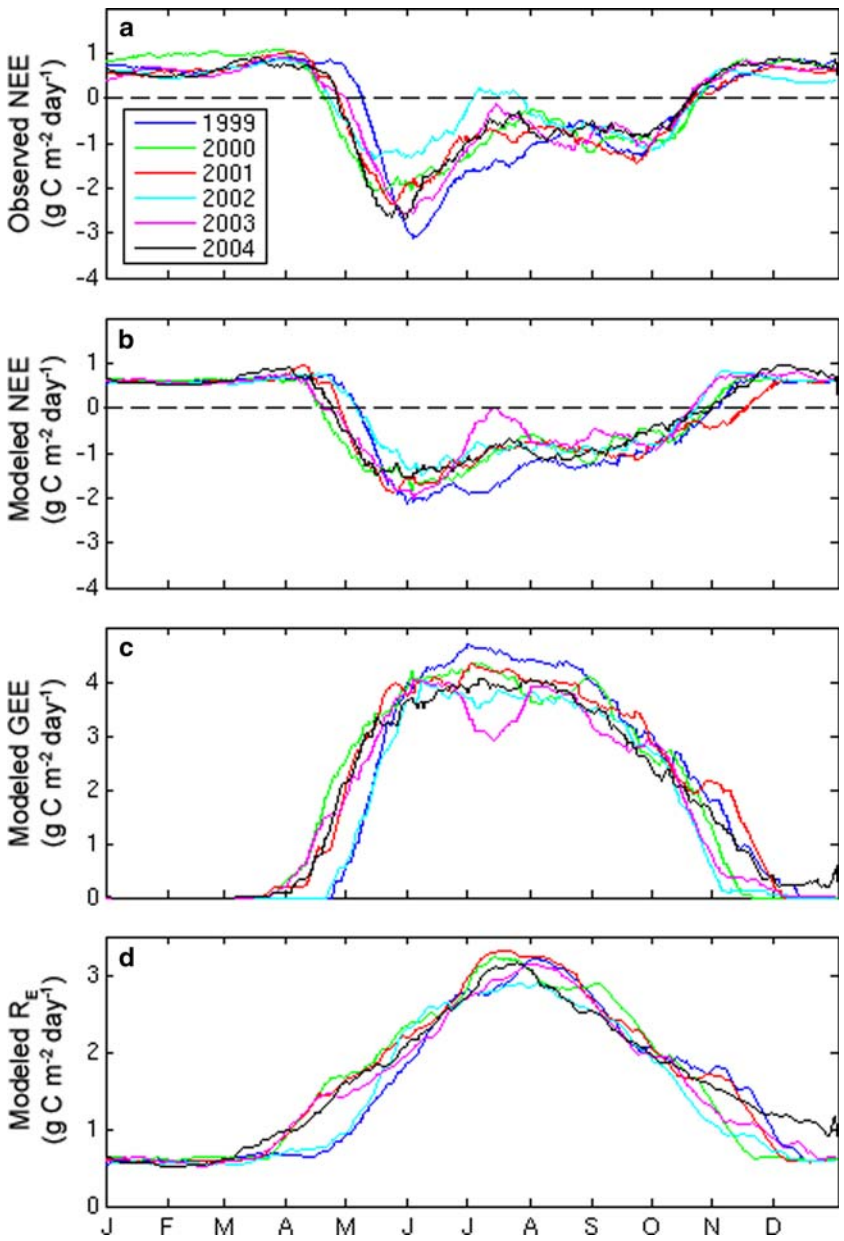

Fig. 3 Observed (**a**) and modeled (**b**) NEE, and modeled GEE (**c**) and R_E (**d**) for the years 1999–2004. By separating NEE into GEE and R_E, we are better able to diagnose causes of the observed interannual variability. Fluxes are shown as running 28-day means

The model predicted that the majority of R_E was autotrophic (R_A), and that only a small fraction was heterotrophic (R_H) (Fig. 4c). The optimized base soil respiration rate (K_H, 0.007 g C g^{-1} C year^{-1}) was almost a factor of ten lower than the initial guess, derived from soil chamber measurements at the site (0.06 g C g^{-1} C year^{-1}; Scott-Denton et al. 2003). While we have reason to believe that the initial guess was too high—and it is for this reason that we specified a wide prior distribution for this parameter—it is unlikely that the initial value was a factor of ten too high. Furthermore, the optimized soil respiration Q_{10} ($Q10_S$, 4.96) was significantly higher than the commonly accepted value of 2. The net effect of these two parameter anomalies was that the model predicted virtually no soil respiration in the cold winter months, and higher, but still relatively low, soil respiration in the summer months (Fig. 4c). In the model, compensation for these low values of R_H occurred through the prediction of relatively high values of R_A. Overall, the model predicted mean respiration fluxes (during the period 1999–2004) of 94 g C m^{-2} year^{-1} R_H and 486 g C m^{-2} year^{-1} R_A.

In order to probe possible biases in the way that the model treats R_H, we performed an experiment in which we held the K_H parameter fixed at two different values: 0.016 g C g^{-1} C year^{-1} and 0.032 g C g^{-1} C year^{-1}. These values were chosen to make annual R_H

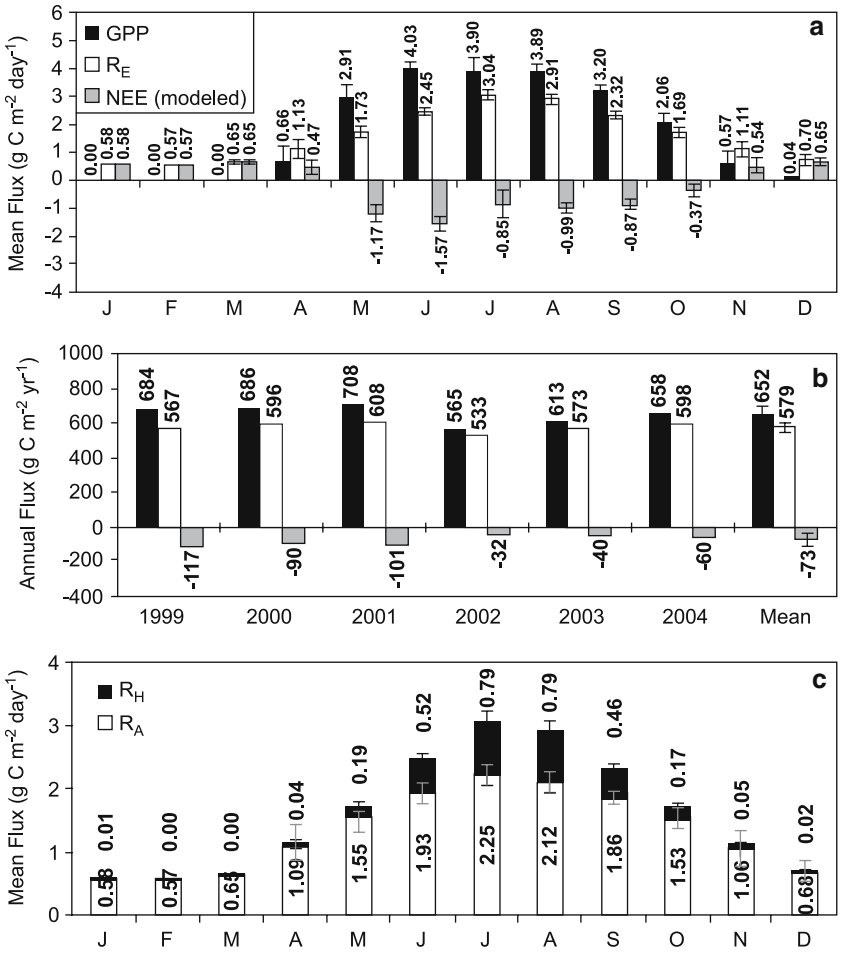

Fig. 4 Optimized breakdown of NEE into its component fluxes, gross photosynthesis (*GEE*) and total ecosystem respiration (R_E), by month (**a**) and by year (**b**), and of total respiration into autotrophic and heterotrophic respiration (**c**). November and December fluxes give means during the period 1998–2004; other months give means for 1999–2004. *Error bars* show interannual variability for each month (**a**, **c**), or for the entire year (**b**) (one standard deviation). The model seems to be able to separate NEE into GEE and R_E well, but does not seem to be able to estimate an accurate separation of R_E into R_A and R_H (see text)

approximately equal to observed, above-ground litterfall and twice-observed, above-ground litterfall, respectively. (Total above-ground litterfall at this site averaged 184 g C m^{-2} year^{-1} over the period 2000–2001; Scott-Denton, University of Colorado, unpublished data.) The higher values of K_H caused increases in annual R_H (Table 4). However, the increases in R_H were less than the increases in K_H because the optimization caused a decrease in $Q10_S$ when forced with higher initial values of K_H: even when K_H was increased by as much as a factor of five, annual R_H increased by less than a factor of two. The optimization protocol seemed to ''favor'' keeping R_H relatively low, so that even when forced with the initial condition of annual R_H equal to twice the observed above-ground litterfall carbon content, the optimized parameterization produced a final solution with R_H slightly less than observed above-ground litterfall.

Despite large perturbations to a key model parameter (i.e., R_H), the GEE/R_E ratio remained approximately the same in the three runs performed for this experiment. Modeled annual R_A decreased to compensate for increases in annual R_H (Table 4). An experiment in which we fixed A_{max}, the maximum photosynthetic rate, at its initial guess value—about 70% greater than its optimized value—gave similar results (data not shown). Here, too, the change in the average GEE/R_E partitioning was negligible, but there was a significant change in the R_A/R_H partitioning, with annual average R_H about 50% higher, and R_A slightly lower than in the control run.

Optimization with different time steps

We performed two experiments to test the optimization's sensitivity to the time scale of the model-data comparisons. First, we investigated how much information is lost by performing model-data comparisons once per day, instead of twice per day as in the standard setup. Second, we investigated how much information is gained by performing model-data comparisons on the original half-hourly fluxes.

Table 4 The effect of holding the base soil respiration rate (K_H) fixed at different values. Modeled fluxes [gross photosynthesis (GEE), total ecosystem respiration (R_E), autotrophic respiration (R_A), heterotrophic respiration (R_H), net primary productivity (NPP), and litterfall] are given as means over the period 1999–2004. All fluxes are in g C m^{-2} $year^{-1}$. Notice that the optimized soil respiration Q_{10} value ($Q10_S$) decreases as K_H increases, dampening the increase in annual R_H with increasing K_H

	Optimized K_H (0.007 g C g^{-1} C $year^{-1}$)	K_H fixed at 0.016 g C g^{-1} C $year^{-1}$	K_H fixed at 0.032 g C g^{-1} C $year^{-1}$
Best log likelihood[a]	–2,727.0	–2,748.0	–2,806.6
RMS error[b]	0.530	0.534	0.543
No. of free parameters	17	16	16
BIC[c]	5,592.6	5,626.4	5,743.6
$Q10_S$ (optimized)	4.96	2.51	1.43
GEE	652	652	653
R_E	579	579	583
R_A	486	447	407
R_H	94	132	176
NPP	167	205	245
Litterfall (model)[d]	265	267	268
Litterfall (obs.)[e]	184	184	184

[a]Larger (i.e., closer to zero) numbers mean greater likelihood

[b]Root mean square error in g C m^{-2} over a single time step, for valid data points only

[c]*BIC* (Bayesian Information Criterion)=–2LL+K ln(n), where LL is the log likelihood, K is the number of free parameters, and n is the number of data points used in the optimization (3,474). A lower BIC indicates a model with greater support from the data (Kendall and Ord 1990)

[d]Includes root turnover as well as above-ground litterfall. The parameters governing this flux in the model were all held fixed in the optimization, at values derived from a variety of field studies (see Table 2)

[e]Above-ground litterfall only. Mean over seven plots and 2 years (2000–2001) (L. Scott-Denton, unpublished data)

Because SIPNET was structured to assimilate daytime and nighttime fluxes separately, and then is optimized on both simultaneously, the optimized model matched the observed diurnal cycle fairly well (Fig. 5). The model slightly underestimated daytime uptake early in the growing season, underestimated nighttime respiration in the summer and tended to overestimate both daytime uptake and nighttime respiration in November, the key month for switching from net monthly CO_2 uptake to net monthly CO_2 loss (Fig. 5a). This resulted in a consistent negative bias in the model's prediction of annual nighttime respiration, but little bias in the model's prediction of annual daytime CO_2 uptake; overall, this resulted in a slight overestimate of net CO_2 uptake relative to the observations (Fig. 5b). However, the biases that exist are small, and this lends support to the model's separation of GEE and R_E.

We evaluated the model structure with regard to diurnal information on parameter retrieval by aggregating modeled and observed fluxes to a daily time step before performing the model-data comparison. The model was still run at the same twice-daily resolution, so the driving meteorological data remained the same. With this aggregation, the model still predicted total NEE well, but significantly underestimated both daytime uptake and nighttime respiration during the growing season (Fig. 6; cf. Fig. 5a).

We performed an additional optimization in which we used the half-hourly meteorological and flux data to test the possibility that some aspects of model-data mismatch were caused by temporal resolution. This half-hourly optimization led to a few significant differences in retrieved parameter values (Table 3). The most significant difference was in the $PPFD_{1/2}$ parameter. The increase in $PPFD_{1/2}$ also forced an increase in A_{max} in order to keep average realized GEE from changing too much; this in turn forced a decrease in K_F. The K_{WUE} parameter, governing plant water use efficiency, was also much higher in the half-hourly optimization. However, because the modeled water fluxes were not directly constrained by observations, the parameters governing these fluxes could vary widely in the optimization (Wang et al. 2001; Sacks et al. 2006).

Although the half-hourly optimization had the capacity to capture more nonlinearities in the ecosystem's response to environmental drivers, it actually led to about a 5% *increase* in the RMS model-data error (after aggregating from the half-hourly time steps to a twice-daily time step). Furthermore, the half-hourly optimization led to only small improvements in the major areas of model-data misfit, estimating slightly greater peak summertime uptake and peak nighttime respiration than the twice-daily optimization. The flux partitioning was similar in the half-hourly optimization,

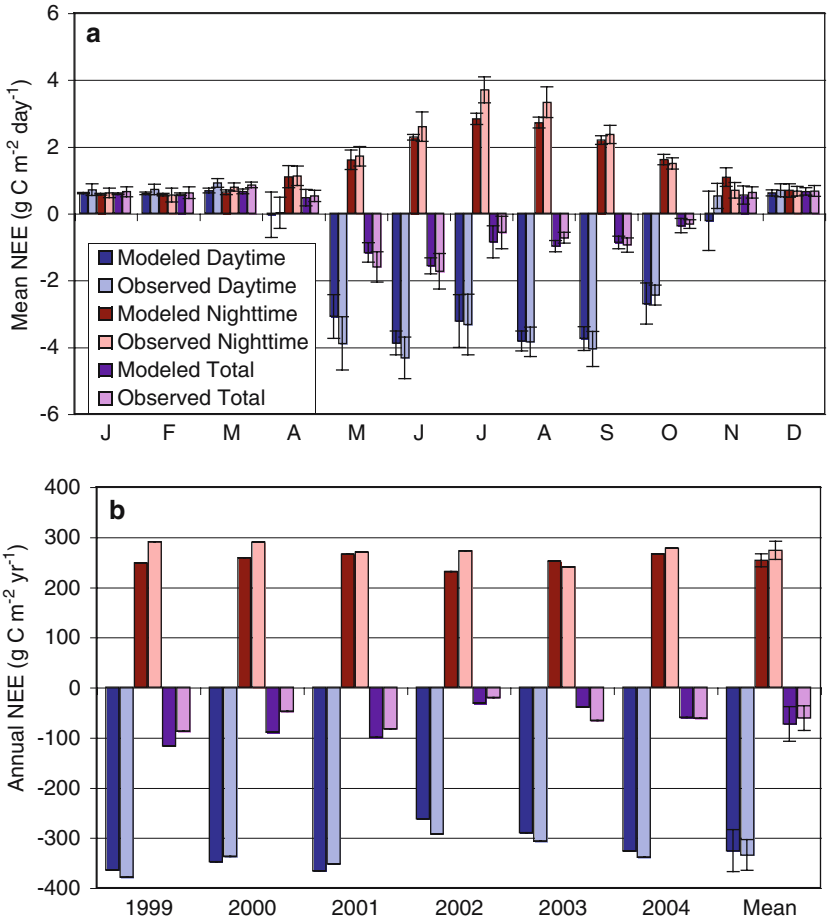

Fig. 5 Modeled and observed mean fluxes by month (**a**) and year (**b**), broken down into day and night. *Error bars* show interannual variability for each month (**a**) or for the entire year (**b**) (one standard deviation). Because we ran and optimized the model at a twice-daily (daytime and nighttime) time step, the optimized model fit the observations fairly well both during the day and at night. This lends support to our partitioning of NEE into GEE and R_E

with about a 5% increase in the estimated values of both GEE and R_E. The estimated value of R_H increased by 33%, but was still too low.

Discussion

Model-data fusion is a relatively new approach to data and model analysis that provides a high level of empirical constraint over model predictions, while at the same time probing model structure and parameter relationships for the source of model-data mismatch (Schulz et al. 2001; Wang et al. 2001; Braswell et al. 2005; Raupach et al. 2005; Williams et al. 2005; Sacks et al. 2006). Model-data fusion holds great promise as a tool to partition the photosynthetic and respiratory components of NEE, and study their separate responses to environmental control. The assimilation system that we used successfully separated GEE and R_E; the separation into component fluxes was based on variations in the observations themselves and process-level understanding, as embodied in the model. There was good agreement between the model predictions and observations of NEE at both the seasonal and interannual time scales.

When the model was fit to total daily NEE, as opposed to separate day and night NEE, it predicted seasonal and interannual patterns of NEE equally well, but for the wrong reasons. While modeled daily NEE remained within the uncertainty of the observations, it arose from greatly underestimated fluxes of both GEE and R_E. Since the total diurnal and separated day/night model structures were identical, differences in their predictions of GEE and R_E were due solely to differences in parameter values.

The results of the above experiment have implications for using daily or longer estimates of NEE to validate ecosystem models. Eddy covariance data are often aggregated to longer time scales to produce estimates that are less uncertain than the individual half-hourly measurements; however, aggregation to the daily, weekly, and longer time scales reduces the information content of the data. As an alternative, separate aggregation of the daytime and nighttime hours to daily and longer time scales should be considered (Figs. 5, 6). This produces robust time integrals

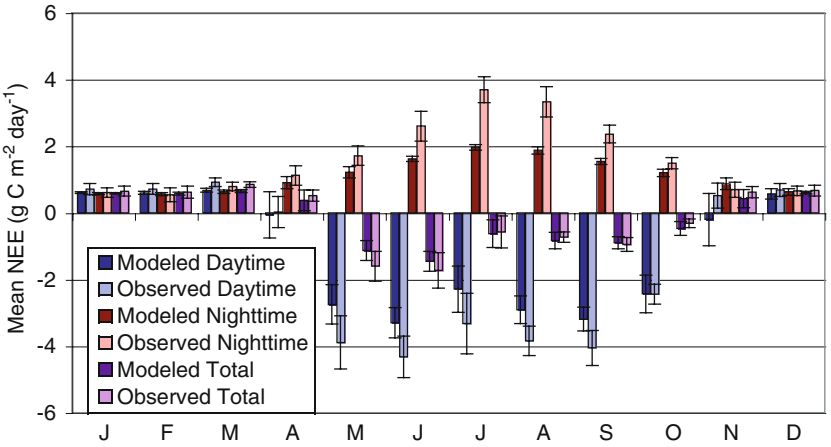

Fig. 6 Modeled and observed mean fluxes by month, broken down into day and night, for an optimization in which we aggregated the observations up to a daily time step, no longer separating day and night. *Error bars* show interannual variability for each month (one standard deviation). When such an aggregation is performed, the model is unable to match the correct diurnal cycle of the observations and, thus, incorrectly predicts both GEE and R_E

while allowing a degree of independent assessment of GEE and R_E.

However, little advantage was gained using half-hourly observations to run and optimize the model. Most model processes are sensitive primarily to environmental variations on time scales greater than 30 min. The main reason to use these short time steps would be to estimate parameters associated with photosynthetic physiology or transpiration, which are sensitive to diurnal variation in light and humidity.

There is a trend toward adopting carbon models that use short time steps (seconds to minutes); the reductionist assumption driving this trend is that shorter time steps will permit greater mechanistic realism. The principal challenge in moving models toward these shorter time steps is that the seconds-to-minutes environmental information required to drive the models is difficult to obtain. However, even with the necessary meteorological drivers, it is not always advantageous to run the model at these shorter time steps. As the difference in the retrieved values of the $PPFD_{1/2}$ parameter illustrates (Table 3), an ecosystem's sensitivity to environmental conditions can vary with the time scale under consideration. A model that is designed to perform well on a short time scale will not necessarily perform well on longer time scales.

The modeled separation of heterotrophic and autotrophic respiration was far less satisfactory than the overall separation of NEE into GEE and R_E. While the day–night contrast allows some independent estimation of GEE and R_E, flux data contain less embedded information capable of constraining the respiratory separation. This separation relies primarily on subtle differences between the correlation of NEE with air temperature and with soil temperature. If the system is close to steady state, then heterotrophic respiration should be close to the sum of above-ground litterfall and below-ground root turnover. Although this system is not in steady state, it is almost certainly closer to steady state than is suggested by this analysis.

At Niwot Ridge, longer growing seasons decrease carbon uptake. In this subalpine ecosystem, one of the principal determinants of annual NEE is the length of the spring snow-melt period, and the magnitude of NEE during this period (Monson et al. 2002, 2005). Early spring warming tends to be correlated with shallow late-spring snow pack and, as a result, low springtime and annual net CO_2 uptake. This was confirmed in the current study, in which a longer growing season (defined as the interval between the spring onset of net negative NEE and the fall transition back to positive NEE: the interval between zero crossings) due to an early spring warm-up was associated with a decreased annual net CO_2 uptake, by an average of 1.37 g C m^{-2} day^{-1} using the observed NEE (Fig. 7) (the relationship using modeled NEE was similar). The

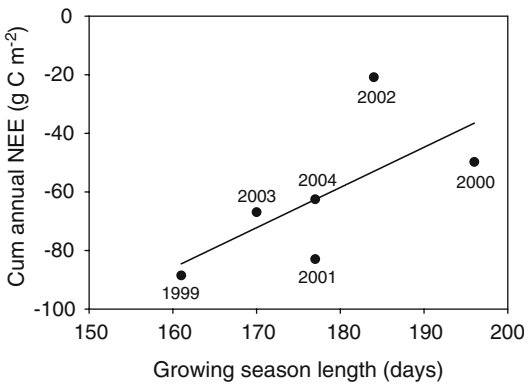

Fig. 7 Relationship between growing season length and observed cumulative annual NEE, 1999–2004. "Growing season length" is defined here as the interval between the spring onset of net negative NEE and the fall transition back to positive NEE: the interval between zero crossings. Longer growing seasons are associated with *less* annual CO_2 uptake, probably because of the effects of snow-melt timing on water availability. The best-fit line, shown here, is given by the equation $y=1.37x–305$ ($R^2=0.45$)

model-data fusion's partitioning of NEE into its components showed that variability in GEE explained 56% and 80% of the year-to-year variation in observed and modeled NEE, respectively. Thus, we surmised that growing season length affects NEE primarily through its influence on GEE, and particularly through the relationship between the timing of snow-melt and growing season water availability.

Churkina et al. (2005) recently showed that a strong relationship exists between the carbon uptake period (defined as the number of days per year with negative NEE) and annual NEE across many evergreen needleleafed sites from the FLUXNET network. The slope of that relationship, determined among many separate sites, was larger than the relatively weak interannual response at our single site (data not shown). This is in accordance with the prediction of Churkina et al. (2005) that the year-to-year response at a single site should differ from that determined across broader spatial scales. Thus, the spatial and interannual responses of NEE to growing season length should not be equated.

Different measures of the length of the growing season or photosynthetic period produced strikingly different, though ultimately consistent, conclusions. At Niwot Ridge, the length of the carbon uptake period (days of negative NEE) was inversely correlated with the growing season length (the interval between the spring and fall zero crossings) (data not shown). Thus, years with earlier springs had more days with positive daily NEE (carbon efflux) during the growing season, i.e., warm springs tend to lead into summers with increased stress. All else being equal, these two measures should be positively correlated, but at Niwot, the tendency is for an inverse correlation. This tendency is likely a result of three factors: first, one cause of early spring is a low snow pack which means low water availability; second, warm springs may alter hydrological partitioning, increasing runoff and evaporation and decreasing the water available for transpiration; third, climatologically warm springs have been correlated with warm summers, possibly increasing stress and reducing carbon uptake.

Interactions between temperature and moisture are important. For example, the spring of 2004 supported a relatively high rate of CO_2 uptake despite a warm temperature anomaly; however, it also had a large positive precipitation anomaly. Conversely, the spring of 2003 supported a high rate of CO_2 uptake despite a dry precipitation anomaly; however, it also had a cold temperature anomaly. In broad terms, it appears that temperature and precipitation anomalies can compensate for each other. A deep spring snow pack can override the negative effects of warm temperature, and low spring temperatures can override the negative effects of a shallow snow pack. The model-data fusion that we employed correctly identified the major carbon flux anomalies associated with spring variability, agreeing with the observations that carbon uptake began earliest in 2000, latest in 1999, and at similar times in 2001, 2002, 2003 and 2004 (Fig. 3a, b).

Model-data fusion techniques applied to long eddy covariance time series can illuminate the impact of climate on NEE, GEE and R_E. Our analysis has revealed that, in general, warmer conditions during the growing season at the Niwot Ridge forest will increase GEE and NEE only if adequate moisture is present. Predictions of impacts of temperature changes on carbon balance will depend critically on the assumptions made about the hydrological cycle. If warmer conditions result in a shorter snow-melt period, then warming will likely reduce net CO_2 uptake. Conversely, if warming is accompanied by an intensified hydrological cycle (Trenberth et al. 2003) with increased winter or summer precipitation, GEE and net uptake could increase.

Acknowledgments Rob Braswell provided much of the impetus for the SIPNET modeling and helped us develop many of the ideas that led to this study; we are grateful for his intellectual contributions. We are also grateful for Ernst Linder's help with the statistics underlying the parameter estimation. We thank Sean Burns, Andrew Turnipseed, Laura Scott-Denton and others who were instrumental in the data collection. Thanks also to Galina Churkina for insights into growing season length. Finally, we thank three anonymous reviewers for their constructive comments. This work was supported by grants from the National Aeronautics and Space Administration (TE/02-0000-0015 & NAG5-12876), the National Science Foundation (2003108), the National Oceanic and Atmospheric Administration (2002192), and a grant from the South Central Section of the National Institute for Global Environmental Change (NIGEC) through the US Department of Energy (BER Program) (Cooperative Agreement No. DE-FC03-90ER61010). The National Center for Atmospheric Research is funded by the National Science Foundation. The experiments performed for this study comply with the current laws of the United States of America.

References

Aber JD, Federer CA (1992) A generalized, lumped-parameter model of photosynthesis, evapotranspiration and net primary production in temperate and boreal forest ecosystems. Oecologia 92:463–474

Aber JD, Ollinger SV, Federer CA, Reich PB, Goulden ML, Kicklighter DW, Melillo JM, Lathrop RG (1995) Predicting the effects of climate change on water yield and forest production in the northeastern united states. Clim Res 5:207–222

Aber JD, Reich PB, Goulden ML (1996) Extrapolating leaf CO_2 exchange to the canopy: a generalized model of forest

photosynthesis compared with measurements by eddy correlation. Oecologia 106:257–265
Aber JD, Ollinger SV, Driscoll CT (1997) Modeling nitrogen saturation in forest ecosystems in response to land use and atmospheric deposition. Ecol Model 101:61–78
Angert A, Biraud S, Bonfils C, Henning CC, Buermann W, Pinzon J, Tucker CJ, Fung I (2005) Drier summers cancel out the CO_2 uptake enhancement induced by warmer springs. Proc Natl Acad Sci U S A 102:10823–10827
Baldocchi DD (2003) Assessing the eddy covariance technique for evaluating carbon dioxide exchange rates of ecosystems: past present and future. Glob Change Biol 9:479–492
Braswell BH, Sacks WJ, Linder E, Schimel DS (2005) Estimating diurnal to annual ecosystem parameters by synthesis of a carbon flux model with eddy covariance net ecosystem exchange observations. Glob Change Biol 11:335–355
Breshears DD, Cobb NS, Rich PM, Price KP, Allen CD, Balice RG, Romme WH, Kastens JH, Floyd ML, Belnap J, Anderson JJ, Myers OB, Meyer CW (2005) Regional vegetation die-off in response to global-change-type drought. Proc Natl Acad Sci U S A 102:15144–15148
Churkina G, Schimel D, Braswell BH, Xiao XM (2005) Spatial analysis of growing season length control over net ecosystem exchange. Glob Change Biol 11:1777–1787
Ciais P, Reichstein M, Viovy N, Granier A, Ogee J, Allard V, Aubinet M, Buchmann N, Bernhofer C, Carrara A, Chevallier F, De Noblet N, Friend AD, Friedlingstein P, Grunwald T, Heinesch B, Keronen P, Knohl A, Krinner G, Loustau D, Manca G, Matteucci G, Miglietta F, Ourcival JM, Papale D, Pilegaard K, Rambal S, Seufert G, Soussana JF, Sanz MJ, Schulze ED, Vesala T, Valentini R (2005) Europe-wide reduction in primary productivity caused by the heat and drought in 2003. Nature 437:529–533
Goulden ML, Munger JW, Fan SM, Daube BC, Wofsy SC (1996) Measurements of carbon sequestration by long-term eddy covariance: methods and a critical evaluation of accuracy. Glob Change Biol 2:169–182
Hollinger DY, Goltz SM, Davidson EA, Lee JT, Tu K, Valentine HT (1999) Seasonal patterns and environmental control of carbon dioxide and water vapour exchange in an ecotonal boreal forest. Glob Change Biol 5:891–902
Hurtt GC, Armstrong RA (1996) A pelagic ecosystem model calibrated with BATS data. Deep Sea Res Pt II 43:653–683
Kaimal JC, Finnigan JJ (1994) Atmospheric boundary flows: their structure and measurement. Oxford University Press, New York
Kendall MG, Ord JK (1990) Time series. Oxford University Press, New York
Metropolis N, Rosenbluth AW, Rosenbluth MN, Teller AH, Teller E (1953) Equation of state calculations by fast computing machines. J Chem Phys 21:1087–1092
Monson RK, Turnipseed AA, Sparks JP, Harley PC, Scott-Denton LE, Sparks K, Huxman TE (2002) Carbon sequestration in a high-elevation, subalpine forest. Glob Change Biol 8:459–478
Monson RK, Sparks JP, Rosenstiel TN, Scott-Denton LE, Huxman TE, Harley PC, Turnipseed AA, Burns SP, Backlund B, Hu J (2005) Climatic influences on net ecosystem CO_2 exchange during the transition from wintertime carbon source to springtime carbon sink in a high-elevation, subalpine forest. Oecologia 146:130–147
Raupach MR, Rayner PJ, Barrett DJ, DeFries RS, Heimann M, Ojima DS, Quegan S, Schmullius CC (2005) Model-data synthesis in terrestrial carbon observation: methods, data requirements and data uncertainty specifications. Glob Change Biol 11:378–397
Ryan MG, Law BE (2005) Interpreting, measuring, and modeling soil respiration. Biogeochemistry 73:3–27
Sacks WJ, Schimel DS, Monson RK, Braswell BH (2006) Model-data synthesis of diurnal and seasonal CO_2 fluxes at Niwot Ridge, Colorado. Glob Change Biol 12:240–259
Schulz K, Jarvis A, Beven K, Soegaard H (2001) The predictive uncertainty of land surface fluxes in response to increasing ambient carbon dioxide. J Clim 14:2551–2562
Scott-Denton LE, Sparks KL, Monson RK (2003) Spatial and temporal controls of soil respiration rate in a high-elevation, subalpine forest. Soil Biol Biochem 35:525–534
Scott-Denton LE, Rosenstiel TN, Monson RK (2006) Differential controls over the heterotrophic and rhizospheric components of soil respiration in a high-elevation, subalpine forest. Glob Change Biol 12:205–216
Sellers PJ, Heiser MD, Hall FG (1992) Relationship between surface conductance and spectral vegetation indices at intermediate (100 m^2–15 m^2) length scales. J Geophys Res FIFE Spec Issue 97:19033–19060
Sellers PJ, Randall DA, Collatz GJ, Berry JA, Field CB, Dazlich DA, Zhang C, Collelo GD, Bounoua L (1996) A revised land surface parameterization (SiB2) for atmospheric GCMs. 1. Model formulation. J Clim 9:676–705
Trenberth KE, Dai AG, Rasmussen RM, Parsons DB (2003) The changing character of precipitation. Bull Am Meteorol Soc 84:1205–1217
Turnipseed AA, Blanken PD, Anderson DE, Monson RK (2002) Energy budget above a high-elevation subalpine forest in complex topography. Agric Forest Meteorol 110:177–201
Turnipseed AA, Anderson DE, Blanken PD, Baugh WM, Monson RK (2003) Airflows and turbulent flux measurements in mountainous terrain. Part 1: canopy and local effects. Agric Forest Meteorol 119:1–21
Turnipseed AA, Anderson DE, Burns S, Blanken PD, Monson RK (2004) Airflows and turbulent flux measurements in mountainous terrain. Part 2: mesoscale effects. Agric Forest Meteorol 125:187–205
Wang YP, Leuning R, Cleugh HA, Coppin PA (2001) Parameter estimation in surface exchange models using nonlinear inversion: how many parameters can we estimate and which measurements are most useful? Glob Change Biol 7:495–510
Webb EK, Pearman GI, Leuning R (1980) Correction of flux measurements for density effects due to heat and water vapor transfer. Q J R Meteorol Soc 106:85–100
Williams M, Schwarz PA, Law BE, Irvine J, Kurpius MR (2005) An improved analysis of forest carbon dynamics using data assimilation. Glob Change Biol 11:89–105